VOL. 16, NO. 1, 2017, 22-29
www.fke.utm.my/elektrika
ISSN 0128-4428

ELEKTRIKA
Journal of Electrical Engineering

Micromachining Techniques for Millimeterwave Applications: A Short Review

N.A Murad*, M. Esa , M. Sabri, and M. K. A. Rahim

Faculty of Electrical Engineering, Universiti Teknologi Malaysia, 81310 UTM Skudai, Johor, Malaysia.

*Corresponding author: asniza@fke.utm.my , Tel: 607-5557307, Fax: 607-5566262

Abstract: Millimeterwave frequency range gained interest due to the demands on bandwidth and speed in telecommunication system. As the frequency increases, the wavelength is shorter and the devices shrink. To some extent, it is difficult to fabricate the small structure using conventional method. A proper consideration on the manufacturing tolerances is needed in fabricating compact structure precisely as well as minimizing losses and crosstalks between lines in a circuit. Many techniques with different tolerances were discussed. Micromachining is one of the techniques with potential to achieve small structures with great accuracy. This paper presents a short review on micromachining techniques used to manufacture small devices precisely. The techniques discussed are bulk micromachining, LIGA, membrane technology, surface micromachining as well as thick photoresist technique. The process for each technique may differ as well as the tolerances

Keywords: Millimeterwave, micromachining, SU-8 photoresist, LIGA, membrane technology.

© 2017 Penerbit UTM Press. All rights reserved

1. INTRODUCTION

Demands on bandwidth and high data rate communications increased an interest in millimeterwave frequency research work. Planar circuit has served microwave devices for decades. However, at high frequencies, couplings in planar circuits became an issue. Thus, at millimeterwave, a signal confined transmission lines such as coaxial line and waveguide are preferred. The challenge at millimeterwave is the fabrication tolerance with the short wavelength in order to prevent cross talk between signal paths and difficulties in routing multiple lines [1]. Conventional metal milling may still be used, but at very high accuracy, which increases the equipment cost. Microfabrication is a parallel process suitable for large scale production at lower cost than conventional milling.

In order to realize low loss structures, different approaches to overcome high attenuation on passive components at millimeterwave were investigated. One of the approaches involved the use of highly resistive silicon in order to reduce the substrate losses. However, fabrication in standard metal oxide semiconductor (CMOS) use low resistivity silicon [2]. Another approach is micromachining.

Micromachining and microelectromechanical systems (MEMS) evolved from integrated circuit and microsystem technology. MEMS components can be considered micromachined components. However, manufactured micromachined components without reconfigurable actuators involved in converting a control voltage or current into mechanical movement cannot be considered MEMS components [3]. In the late 1980's researchers referred to micromachining as a field that focused on the use of silicon [4]. Nowadays, micromachining has evolved with various techniques.

Micromachining has grown in popularity due to its potential to achieve small structures with great accuracy at a reduced cost. Micromachined transmission lines, high-Q resonators, filters and antennas are categorised in one of four distinct areas in radio-frequency (RF) microelectromechanical systems (MEMS) research [5]. The other three are: 1) RF MEMS switches, varactors and inductors; 2) thin film bulk acoustic resonators and filters; and 3) RF micromechanical resonators and filters.

Micromachining techniques can be categorized into bulk micromachining or surface micromachining. Bulk micromachining consists of wet and dry etching, and photoresist technologies. Photoresist technologies involve photolithography using either X-ray or ultraviolet (UV) light sources. Bulk micromachining, as well as surface micromachining, is also used in membrane technology. The surface micromachining process involves thin film growth on the surface of a substrate. The differences between bulk and surface micromachining are presented in [6]. The thickness of the wafer used determines the vertical dimension of the bulk micromachined structures, which is between 100 to 500 μm. However, in surface micromachined structures, the vertical dimension is determined from the practical thickness of thin film that can be deposited, which is between 0.5 and 2 μm [6]. .

2. BULK MICROMACHINING

The main process in bulk micromachining is the etching. There are two etching techniques; wet etching and dry

etching [7]. The advantage of wet etching is that more than one wafer can be processed at a time. However, dry etching is preferred in achieving vertical walls. The extent of the etching can be controlled by using layers of different materials. The changes of material that determine the depth of etching is called the etch stop [8]. There are three ways of implementing etch stop [8]: 1) silicon-on-insulator (SOI) wafer where different materials are grown layer by layer on one side of a wafer; 2) doping on material; and 3) electrochemically by applying a voltage across a p-n junction that prevents some etchants from affecting the n-type material.

Wet etching can be either isotropic or anisotropic. Isotropic requires etching to progress at the same rate in all directions. For silicon etching, a hydrofluoric, nitric and acetic acid (HNA) etch system is commonly used. A mixture of nitric acid (HNO_3) and hydrofluoric acid (HF) is diluted with water or acetic acid. Isotropic etching can be done at room temperature at a faster rate compared to anisotropic etching [7]. However, isotropic etching is used less frequently than anisotropic [8]. This is because the isotropic etchant attacks a wide area around the structure and consequently may weaken the performance of the device. An example of cantilever design with isotropic and anisotropic etching is shown in Figure 1 (a) and (b), respectively [8]. The figures show that the isotropic etching etched a massive area around the structure.

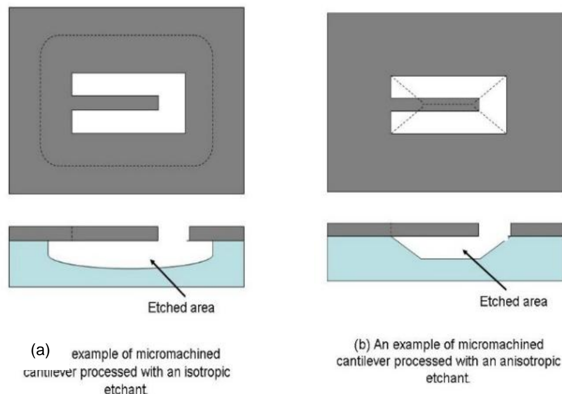

Figure 1. Isotropic and anisotropic etched cantilever structure [8].

Anisotropic etching is restricted by the crystalline structure of the material used and usually has different etching rates in different directions. A solution of potassium hydroxide (KOH) mixed with water, and sometimes with the addition of alcohol, is the most commonly used etchant. The silicon etch rate is influenced by the process temperature [7].

In contrast to wet etching, dry etching needs sophisticated equipment. It is normally done in an evacuated chamber where plasma is generated and used to etch the silicon substrate. Deep Reactive Ion Etching (DRIE) is the most common dry etching process. The wafer is exposed alternately to an etchant and passivant to control the side wall of the structure. The etchant is the plasma of sulphur hexafluoride (SFC), while the passivant is octafluorocyclobutane (C_4F_8). This technique requires expensive equipment and is not efficient for etching layers approximately 0.5 mm and above [9].

As an example, the DRIE process was implemented in fabricating W-band waveguide in [10]. The process is shown in Figure 2. The silicon substrate was cleaned before both sides were deposited by SiO_2. The top SiO_2 layer, which was 3.5 µm thick, was used as a mask for deep silicon etching while the bottom layer, at 0.6 µm, was used as the etch stop. A photoresist layer was deposited on top of the SiO_2 mask layer (Figure 2 (a)). The photoresist was developed and the SiO_2 was patterned (Figure 2 (b)). The silicon substrate layer was etched using the DRIE BOSCH process. The etch stop layer determined the depth of the etching (Figure 2 (c)). The SiO_2 layers were then removed before the silicon substrate was metallised by sputtering Ti and Cu.

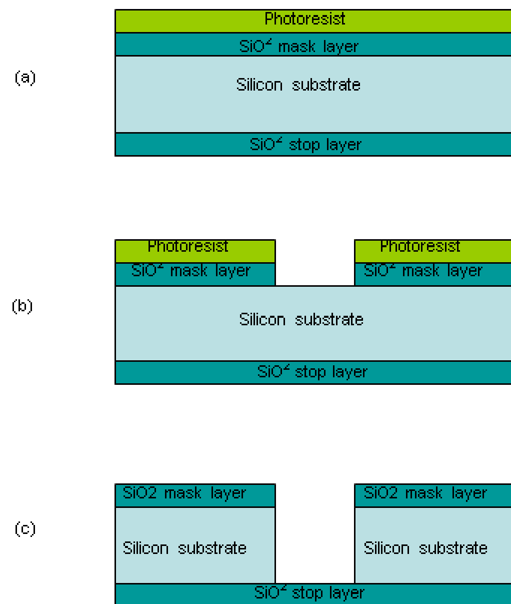

Figure 2. DRIE manufacturing technique [10].

3. LIGA

LIGA is a German acronym for lithography, electroforming and moulding [8]. It can be categorised into two fabrication technologies. One is X-ray LIGA which uses X-rays produced by a synchrotron and the second is UV LIGA which uses ultraviolet light. X-ray light has a higher resolution and a shorter wavelength and is able to create high aspect ratio structures with parallel and smooth side walls. However, it is more expensive compared to ultraviolet (UV) light sources.

Figure 3 shows the principal fabrication steps of UV LIGA [11]. A thick photoresist layer is exposed before being developed (Figure 3 (a)). For X-rays, a special sophisticated mask is required for this process step. For UV LIGA a chromium mask can be used. The photoresist is developed (Figure 3 (b)) to be used as a mould for galvanoforming (Figure 3 (c)) or electroforming where material is deposited by means of an electric current or by means of reactive chemical mixtures. Components are created by electro-deposition when the photoresist mould gap is filled with filling material. Finally, the photoresist is stripped away, leaving the metal structure (Figure 3

(d)). The released components can be used for injection moulding.

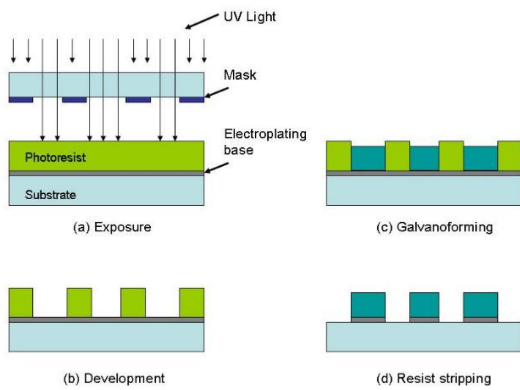

Figure 3. UV LIGA fabrication steps [11].

4. MEMBRANE TECHNOLOGY

Membrane technology in micromaching first gained attention due to its ability to produce thick pieces at high aspect ratios [12]. A thin layer of high quality dielectric material is applied to support a suspended structure. The etch stop discussed earlier is very useful in fabricating membranes. Membrane technology is commonly used in integrating micromachined transmission lines and antennas. In antenna design, the idea is to have a cavity underneath the radiator, thus reducing the effective permittivity of the substrate and consequently minimising losses due to surface waves. For instance, a membrane supported patch antenna was presented in [13]. The manufacturing process is depicted in Figure 4.

The process in Figure 4 starts with a 2 µm layer of SiO2 deposited on the silicon substrate before it was metallised by 3 µm thick Cr and Au on both sides (Figure 4 (a)). Then, the Au layer on the front side was patterned to realise the patch antenna (Figure 4 (b)). The back side was patterned as an open window for the bulk micromachining etching process (Figure 4 (c)). An anisotropic wet etch was applied to remove the silicon substrate underneath the circuit area to obtain a thin layer membrane (Figure 4 (d)). Finally, the Cr layer was patterned (Figure 4 (e)).

Other examples of the implementation of membrane technology are the membrane supported transmission lines and Ka-band microwave filter presented in [14]. The top view of the filter structure and the 3D view of the CPW line on the membrane are shown in Figure 5 and 6, respectively. A 1 µm silicon nitride membrane layer was deposited on a 525 µm thick silicon substrate before part of the substrate underneath the circuit was etched away. The circuit was patterned on the membrane surface. A metallised substrate was bonded to form a ground layer and to support the structure.

Membrane technology is also implemented in the manufacture of MEMS switches. The movable bridge membrane allows the switch to turn on and off. The fabrication usually involves the surface micromachining process, which will be presented in the next section.

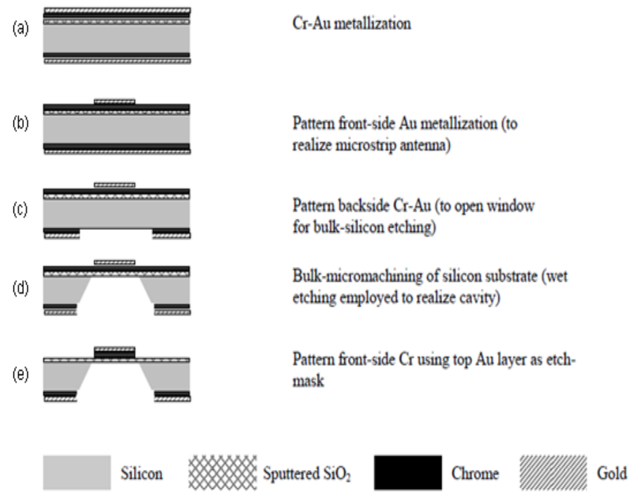

Figure 4. Membrane supported transmission line taken from [13].

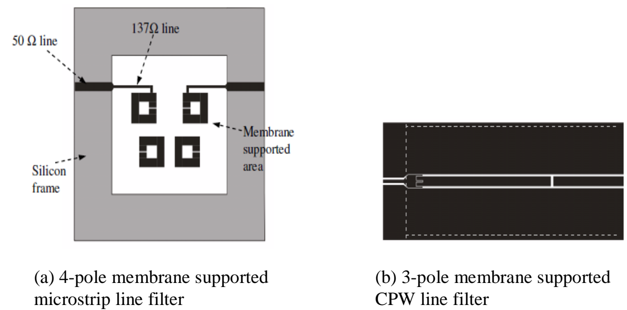

Figure 5. Microwave filters taken from [14].

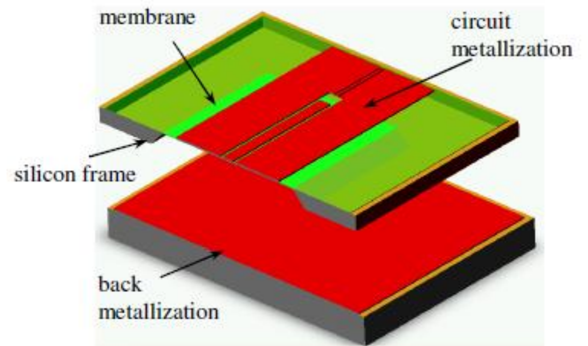

Figure 6. Membrane supported transmission line taken from [14].

4. SURFACE MICROMACHINING

The surface technique selectively adds and removes a deposit film on the wafer [15]. The process involves wet and dry etching together with thin film deposition. The thin film (normally about 1 µm) can be polysilicon, silicon oxide or nitrite. A soluble layer, normally silicon dioxide, is deposited beneath other patterned materials for later removal. The layer is referred to as a sacrificial layer.

A chemical wet etching of the sacrificial layer is the main process in surface micromachining. A soluble or removable sacrificial layer is used to temporarily support

the structural layers during subsequent fabrication steps. It must be stable during deposition and throughout the fabrication process and etched away quickly during the release step. The sacrificial layer can be metal (such as Au, Ni or Al), dielectric (SiO2 or Si3N4), polymer (photoresist or polymethyl) or polyimide [7].

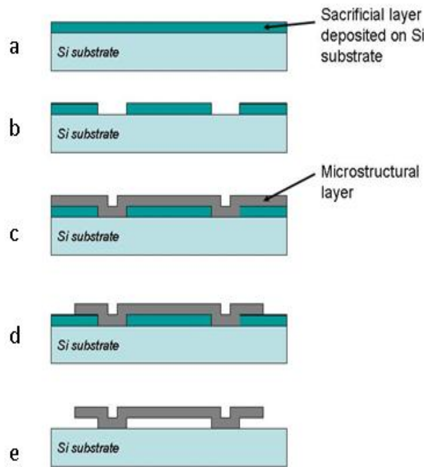

Figure 7. An example of surface micromachining process steps [16].

An example of the surface micromachining steps is illustrated in Figure 7 [16]. A silicon substrate was deposited with a sacrificial layer and coated with a dielectric layer as an isolation layer (Figure 7 a). Then, the layer was patterned with the first mask (Figure 7 b) before a microstructural thin film layer was deposited (Figure 7 b). The microstructural layer, the layer that forms the structure, should be designed with good mechanical and electrical properties. The layer was patterned with a second mask (Figure 7 d) before being released with an etching step to remove the sacrificial layer (Figure 7 e).

Surface micromachining was used in the manufacture of an RF MEMS capacitive switch in [17]. The process is depicted in Figure 8. A 1 μm thick SiO2 layer was grown on the substrate before the switch electrode was patterned from 0.4 μm thick deposited metal and insulated by a layer of patterned PECVD (Plasma Enhanced Chemical Vapour Deposition) silicon nitride (Figure 8 (a)). The insulation was for DC isolation. A 4 μm thick layer of aluminium alloy was evaporated and patterned to define the metal transmission line and the mechanical support before a sacrificial layer was applied and planarized to get a planar and smooth layer (Figure 8 (b)). Then, an aluminium membrane layer less than 0.5 μm was deposited and patterned to form the switch membrane (Figure 8 (c)). The membrane bridge was released by using the plasma etching process (Figure 8 (d)). Without any potential applied, the bridge will remain suspended. The bridge will be pulled down to the dielectric covered metal electrode when the application of an electrostatic field between the bridge and the electrode is strong enough. This creates a capacitive connection between the CPW centre conductor and the ground planes.

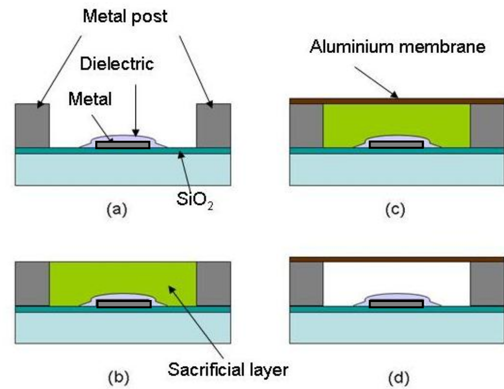

Figure 8. Capacitive switch fabrication process taken from [17].

5. THICK PHOTORESIST

Thick photoresist became popular nowadays in order to get high aspect ratio for precise manufactured devices. The photoresist can be a sacrificial layer or remain as part of the struture. The latter is presented here. The patterned photoresist pieces are coated with metal and assembled to form the structure. It is different from other processes such as LIGA where the photoresist acts as a mould and is removed at the end of the process.

SU-8 is a negative epoxy based photoresist, initially developed by IBM for MEMS applications [18]. It has become of interest for high-aspect ratio (HAR) and three-dimensional (3D) lithography patterning due to its outstanding coating processing properties. Furthermore, it is mechanically and chemically stable, making it suitable for permanent use applications. Thick SU-8 photoresist technique has been adopted in [21-23] and [25-27].

A normal process in thick SU-8 photoresist micromachining typically involves the following steps: spin coat, soft bake, expose, post expose bake (PEB) and develop. Once developed, the pieces are coated with metal before being aligned and bonded together to form a structure. The recipe used for 200 μm layer is shown in Table 1 and described below with a diagram of the process in Figure 9.

Table 1. The thick SU-8 micromachining recipe for 200 μm layer thickness

Procedure Steps	Process Parameters
Substrate pre-treatment	200°C for 5 min
SU-8 Dispense	4 ml
Spread	300 rpm for 5 s
Spin Coat	1000 rpm for 30s
Soft Bake	65°C for 10 min. and 95°C for 75 min
Expose	500 mJ
Post Expose Bake	65°C for 2 min. and 95°C for 20 min
Develop	20 minutes in EC solvent
Hard Bake	150°C for 30 min.
Metalise	1.5 μm of Au (Gold)
Alignment and Bonding	Adhesive

The process can be described as follows.

1. Pre-treatment - In order to obtain maximum process reliability, the silicon substrate is pre-treated. It is rinsed with dilute acid followed by water. To dehydrate the surface, it is put on a hotplate at 200°C for 5 minutes.
2. SU-8 Dispense - The process starts with a static dispensation of around 4 ml SU-8 on a 4 inch silicon substrate. The amount for different viscosities can be approximated from the data sheet. However, some optimization has been made to obtain a more accurate level.
3. Spread - The SU-8 is spread with a 300 rpm spin.
4. Spin coat - The SU-8 is spin coated with a 1000 rpm for 30 seconds.
5. Soft bake - A soft pre-bake is stepped from 65°C for 10 minutes to 95°C for 75 minutes on a levelled hotplate. This is done to evaporate the solvent inside the film. The stepping temperature is used to allow the evaporation process to be more controllable at a lower initial bake temperature. This could result in better coating fidelity, reduced bead and better resistance to substrate adhesion [19].
6. Expose – The exposure dose is 500 mJ for a 200 µm thick SU-8 layer. The SU-8 coated silicon and the mask are placed in the mask aligner and exposed to UV light from a mercury lamp.
7. Post Exposure Bake (PEB) – The PEB is done to selectively cross link the exposed portions of the film. Again, a two step hot plate contact process is done to minimize stress, wafer bowing and to resist cracking. The post bake is stepped from 65°C for 2 minutes to 95°C for 20 minutes.
8. Develop – Ethyl lactate solvent is used to develop the SU-8 pieces. The wafer is agitated in the solvent for about 20 minutes before being rinsed with isopropyl alcohol and dried with a gentle stream of air.
9. Hard Bake –The processed wafer is hard baked at 150°C. After 30 minutes, the hotplate is switched off and the wafer is left on the hotplate, allowing it to cool down gradually. This will help to reduce the stress. The hard bake is done to keep the pieces stable during subsequent processing.
10. Metallization – The pieces would be susceptible to bending during this coating process without the hard bake. The SU-8 pieces are first sputter-coated with a 5nm Cr adhesion layer, followed by a1.5 µm thick thermally evaporated gold layer. The thickness of the gold is about five skin depth at 63 GHz, which is thick enough to prevent the signal from penetrating into the SU-8. Skin depth is the distance where the amplitude of the fields in the conductor decays by an amount of 1/e or 36.8 %. It can be calculated by [19]

$$\delta_s = \sqrt{\frac{2}{\omega\mu\sigma}} = \sqrt{\frac{2}{\pi f \mu_0 \sigma}} \quad (1)$$

It can be seen from (1) that the skin depth is inversely proportional to the frequency (f) and the conductance of the material (σ).

11. Bonding – The pieces are aligned and bonded together using a conducting adhesive material.

During the process, some imperfections between the joined layers can be apparent. This can contribute to loss and degradation in the performance of the structure. Losses between each layer may be contributed to by i) excessive or insufficient adhesion material during the bonding process, resulting in imperfect ii) planarization problems, or iii) misalignment between layers during the bonding process. The absence of adhesive mater ial at the edge results in a small cavity on the wall. A second evaporation on the inside wall can be implemented to improve the imperfect wall should one develop during the bonding process. The second evaporation is implemented in [28]. However, it was suggested that further improvement on the fabrication can be done to achieve better performances. Thus,other related improvement was reported such as in [29] for superior performances especially at very high frequencies.

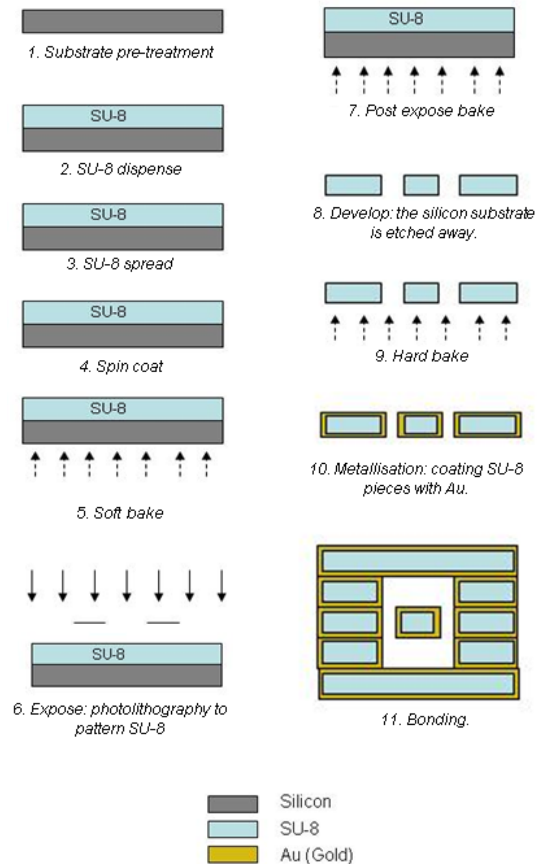

Figure 9. The process of fabrication and assembly.

7. Femtosecond Laser Micromachining

A new technique was developed in the recent years for micromachining for the fabrication of high Q-microdisk, using Femtosecond laser micromachining process relies on different material with a suitable laser pulse energy [31]. The machined process using Femtosecond laser micromachining can be done in less than one minute, and the complete fabrication process can be made as quick as twenty minutes[32]. The micromachining process is

consist of two stages: (1) using Femtosecond laser micromachining for the structure then (2) the surface finishing by using heat reflow.

Fabrication can be made by using Ti sapphire laser system that is produce 100fs pulses with a pulse energy of 10µJ. The Femtosecond Laser micromachining process in this matter is used analogous to a traditional metal lathe with the mechanical cutting tool changed by a focused femtosecond laser. The laser pulse repetition rate is 1 kHz which minimizes thermal heat accumulation when the beam is interrelating with the sample to ensure that material ablation is the only process taking place. The laser is shaped by a horizontal aperture and then focused onto the rotating cylindrical work sample using a 0.2 NA objective lens [31]. Once the high intensity absorbed spot of the laser interacts with the work sample, optical breakdown happens through multi-photon ionization [32].

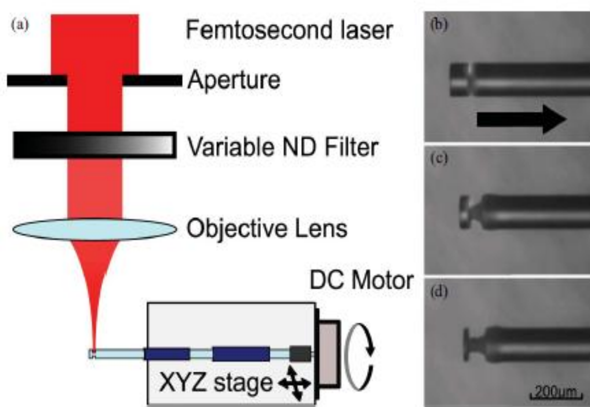

Figure 10. (a) Schematic diagram of micromachining setup. Beam profile is shaped by a horizontal aperture and pulse energy is fine-tuned with a variable neutral density filter. The beam is focused onto the rotating work sample using a 0.2 NA objective lens. (b)– (d) Optical microscope images of the fabrication process. After the initial cut is made, the rotating optical fiber is translated through the focus of the laser in the direction of the arrow, progressively defining the resonators disk structure [32].

This process produces a white-light continuum, but does not affect with the micromachining process. Optical breakdown ablates the material, creating a symmetric channel around the fibre as it is existence rotated. The first cut into the optical fibre is shaped over 100µm away from the tip of the fibre. It is made by carrying the rotating fibre into the focus of the laser, which is fixed in space. The tip of the rotating fibre is then translated along the axis of the fibre toward the fixed focus of the lasers shown in Figure. 10

This procedure forms the disk structure of the micro resonator. The micromachining procedure eliminates only the outer most layer of material as the work sample is being rotated. This tolerates for fabrication of resonators of any diameter specified material convenience. The micromachining process used is a turning process that brings cylindrically symmetric cuts in the work material. The ability to spatially limit the pulse energy perpendicular to the axis of the work sample allows for better quality cutting with an increased tolerance for beam misalignment [33]. At the focus of the objective lens, the spatial profile of the beam resembles the Fourier transform of the input beam profile as demonstrated in Figure 11.

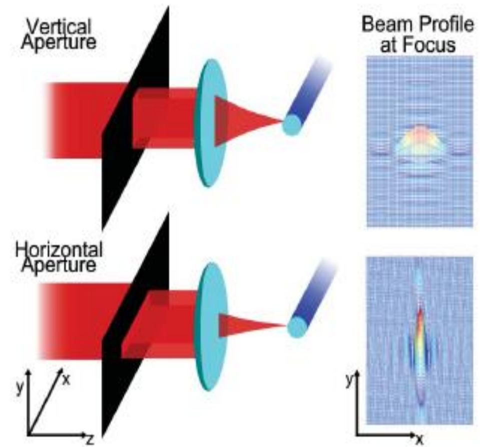

Figure 11. Beam shaped using an aperture to improve the quality of the ablation process. The left image shows the approximate beam profile at the focus of the objective lens on the optical fiber after being shaped by a vertical aperture. The right image shows the approximate beam profile after being shaped by a horizontal aperture. The horizontal aperture creates a beam profile at the focus of the objective lens with the majority of the beam energy localized in the axis of rotation of the optical fiber. This allows for higher quality ablation to occur [32].

8. CONCLUSION

Different micromachining techniques have been presented. Bulk and surface micromachining are mature techniques with the emphasis on the etching process to control the side walls. The bulk micromachining process removes selective parts of the material to form a structure, while surface micromachining forms a structure by growing or adding thin films (0.5 to 2.0 µm) on top of a silicon wafer or other substrate layer. The use of a sacrificial layer in the latter technique lends flexibility to the structure. However, low aspect ratios require a search for different photoresists to obtain precise structures at high aspect ratios [25].

The suitability of fabricating microwave components using three different micromachining technologies were investigated in [18]. The technologies were i) SU-8 photoresist, ii) Si deep reactive ion etching (DRIE), and iii) electroforming. It was claimed that these three technologies were able to produce accurate defined thick pieces [18]. The technologies were used to construct various coaxial lines operating in the 20 GHz to 50 GHz range. Excellent microwave/millimeterwave performance was obtained for SU-8 and etched silicon devices, but not for electroplated Ni ones. In addition, SU-8 was found to produce the most accurate pieces with a deviation angle of 0.15 ° on the lateral sidewall, which is the lowest compared to 0.6 ° obtained from Ni electroplating and 1 ° from DRIE. SU-8 is not only more accurate, but also chemically and thermally stable, with a lower cost. A very thick SU-8 layer can achieve an excellent aspect

ratio of 1:50 [9]. Thus, SU-8 is gaining popularity in manufacturing millimeterwave devices.

ACKNOWLEDGMENT

The author would like to thank Faculty of Electrical Engineering, Universiti Teknologi Malaysia and Emerging Device Technology Group, The University of Birmingham for their support.

REFERENCES

[1] J. R. Reid, V. Vasilyev, and R. T. Webster, "Three dimensional micromachining for millimeter-wave circuits," in *Wireless and Microwave Technology Conference*, 2009, pp. 1-4.

[2] L. L. W. Leung, H. Wai-Cheong, and K. J. Chen, "Low-loss coplanar waveguides interconnects on low-resistivity silicon substrate," *IEEE Transactions on Components and Packaging Technologies,* vol. 27, pp. 507-512, 2004.

[3] S. Lucyszyn, "Review of radio frequency microelectromechanical systems technology," *IEE Proceedings - Science, Measurement and Technology,* vol. 151, pp. 93-103, 2004.

[4] C. Liu, *Foundations of MEMS*: Pearson Education Inc., 2006.

[5] G. B. Rebeiz, *RF MEMS : Theory, Design, and Technology*: John Wiley & Sons, 2003.

[6] P. J. French and P. M. Sarro, "Surface Versus Bulk Micromachining: a Contest for Suitable Applications " *Journal of Micromechanics and Microengineering,* vol. 8, pp. 45-53, 1998.

[7] B. G. Duixian Liu, Ullrich Pfeiffer, Janusz Grzyb, "Advanced Millimeter-wave Technologies," 2009.

[8] R. W. Johnstone and M. Parameswaran, *An Introduction to Surface Micromachining*: Kluwer Academic Publisher, 2004.

[9] Y. Wang, M. Ke, M. J. Lancaster, and F. Huang, "Micromachined Millimeter-wave Rectangular Coaxial Branch-Line Coupler with Enhanced Bandwidth.," *IEEE Transaction on Microwave Theory and Techniques,* vol. 57, pp. 1655-1660, 2009.

[10] L. Yuan, P. L. Kirby, and J. Papapolymerou, "Silicon Micromachined W-Band Folded and Straight Waveguides Using DRIE Technique," in *Microwave Symposium Digest, 2006. IEEE MTT-S International*, 2006, pp. 1915-1918.

[11] Q. Wenmin, C. Wenzel, A. Jahn, and D. Zeidler, "UV-LIGA: a promising and low-cost variant for microsystem technology," in *Conference on Optoelectronic and Microelectronic Materials Devices*, 1998, pp. 380-383.

[12] M. Ke, Yi Wang, Kyle Jiang, M. J. Lancaster, "Micromachined Rectangular Coaxial Line and Cavity Resonator for 77 GHz Applications Using SU8 Photoresist," in *Asia Pacific Microwave Conference, 2008*, Hong Kong, 2008, pp. 1-4.

[13] S. Preeti, K. K. Shiban, and C. Sudhir, "Design and development of microstrip patch antenna at Ka-band using MEMS technology," Proc. SPIE 6172, Smart Structures and Materials, 2006, p. 61721F.

[14] Y. Wang, M. J. Prest, and M. J. Lancaster, "Membrane Supported Transmission Lines and Filters," in *European Microwave Conference* 2008, pp. 1133-1136.

[15] J. M. Bustillo, R. T. Howe, and R. S. Muller, "Surface Micromachining for Microelectromechanical Systems," in *Proceedings of The IEEE*. vol. 86, 1998, pp. 1552-1574.

[16] M. J. Madou, *Fundamentals of Microfabrication : The Science of Miniturization*: CRC Press, 2002.

[17] C. L. Goldsmith, Z. Yao, S. Eshelman, and D. Denniston, "Performance of Low Loss RF MEMS Capacitive Switch," *IEEE Microwave Guided Wave Letter,* vol. 8, pp. 269-271, 1998.

[18] M. L. Ke, Y. Wang, X. Wei, K. Jiang, and M. J. Lancaster, "Precision Microfabrication of Millimetre Wave Components," in *Laser Metrology and Machine Performance IX*, 2009.

[19]D. M. Pozar, *Microwave Engineering*, Third ed.: John Wiley & Sons, 2005.

[20] Y. Wang, M. L. Ke, and M. J. Lancaster, "Micromachined 38 Ghz Cavity Resonator and Filter with Rectangular Coaxial Feed Lines," *IET Microwave Antennas Propagation,* vol. 3, pp. 125-129, 2009.

[21] Y. Wang, M. Ke, and M. J. Lancaster, "Micromachined 38 GHz cavity resonator and filter with rectangular-coaxial feed-lines," *Microwaves, Antennas & Propagation, IET,* vol. 3, pp. 125-129, 2009.

[22] M. Ke, Y. Wang, and M. J. Lancaster, "Design and realisation of low loss air-filled rectangular coaxial cable with bent quarter-wavelength supporting stubs," *Microwave and Optical Technology Letters,* vol. 50, pp. 1443-1446, 2008.

[23] Y. Wang, M. Ke, and M. J. Lancaster, "Micromachined 60 GHz Air Filled Interdigital Bandpass Filter," in *International Workshop on Microwave Filters* Toulouse, France, 2009.

[24] E. Koukharenko, M. Kraft, G. J. Ensell, and N. Hollinshead, "A Comparative Study of Different Thick Photoresist for MEMS applications," *Journal of Material Science : Materials in Electronics,* vol. 16, pp. 741-747, 2005.

[25] N. A. Murad, M. J. Lancaster, Yi Wang, M. L. Ke. "Micromachined Millimeter-wave Butler Matrix with a Patch Antenna Array" Mediterranean Microwave Symposium, Tangiers, Morocco, 2009

[26] N. A. Murad, M. J. Lancaster, Y. Wang, and M. Ke, "Micromachined Rectangular Coaxial Line to Ridge Waveguide Transition," Wireless and Microwave Technology Conference Florida, U. S., 2009.

[27] Murad, N.A; Lancaster, M.J.; Gardner, P.; Ke, M.L.; Wang, Y., "Micromachined H-plane horn antenna manufactured using thick SU-8 photoresist," *Electronics Letters* , vol.46, no.11, pp.743,745, May 27 2010.

[28] Shang, X.; Ke, M.L.; Wang, Y.; Lancaster, M.J., "Micromachined WR-3 waveguide filter with embedded bends," *Electronics Letters* , vol.47, no.9, pp.545,547, April 28 2011

[29] Xiaobang Shang; Maolong Ke; Yi Wang; Lancaster, M.J., "WR-3 Band Waveguides and Filters Fabricated Using SU8 Photoresist Micromachining Technology," *IEEE Transactions*

on Terahertz Science and Technology,, vol.2, no.6, pp.629,637, Nov. 2012

[30] Tian Y, Shang X, Lancaster MJ; "Fabrication of multilayered su8 structure for terahertz waveguide with ultralow transmission loss." Journal of Micro/Nanolithography , MEMS and MOEMS. Vol 13, No. 1, Jan, 2014.

[31] R. R. Gattass and E. Mazur, “Femtosecond laser micromachining in transparent materials,” Nature Photon., vol. 2, no. 4, pp. 219–225, 2011.

[32] Kazunari Tada, Gregory A. Cohoon, Khanh Kieu, Masud Mansuripur, and Robert A. Norwood,” Fabrication of High-Q Microresonators Using Femtosecond Laser Micromachining,” IEEE PHOTONICS TECHNOLOGY LETTERS, VOL. 25, NO. 5, MARCH 1, 2013

[33] J. B. Ashcom, R. R. Gattass, C. B. Schaffer, and E. Mazur, “Numerical aperture dependence of damage and supercontinuum generation from femtosecond laser pulses in bulk fused silica,” J. Opt. Soc. Amer. B, vol. 23, no. 11, pp. 2317–2322, 2012.